

TOWARDS A COMPACT XUV FREE-ELECTRON LASER: CHARACTERISING THE QUALITY OF ELECTRON BEAMS GENERATED BY A LASER WAKEFIELD ACCELERATOR*

S. M. Wiggins[#], M. P. Anania, E. Brunetti, S. Cipiccia, B. Ersfeld, M. R. Islam, R. C. Issac, G. Raj, R. P. Shanks, G. Vieux, G. H. Welsh, D. A. Jaroszynski[†], SUPA, Department of Physics, University of Strathclyde, Glasgow G4 0NG, United Kingdom

W. A. Gillespie, SUPA, Division of Electronic Engineering and Physics, University of Dundee, Dundee DD1 4HN, United Kingdom

A. M. MacLeod, School of Computing and Creative Technologies, University of Abertay Dundee, Dundee DD1 1HG, United Kingdom

Abstract

A high power (900 mJ, 35 fs) laser pulse is focused into a gas jet (length 2 mm) and a monoenergetic electron beam is emitted from the laser-induced plasma density wake behind the laser pulse. The most probable electron beam pointing angle as it exits the gas jet is 8 mrad, rotated 40 degrees from the laser polarisation direction. Pepper-pot measurements place an upper limit of 5.5 pi mm mrad on the normalised emittance. The r.m.s. beam divergence is as low as 2 mrad, which indicates an emittance closer to 1 pi mm mrad. The maximum central energy of the beam is ~90 MeV with a r.m.s. relative energy spread as low as 0.8%. An analysis of this unexpectedly high beam quality is presented and its impact on the viability of a free-electron laser driven by the beam is examined.

However, a major challenge is to improve the beam quality to a point where a free-electron laser (FEL) becomes feasible. Conventional RF accelerators routinely deliver beams of high charge density, low emittance, low energy spread as drivers of the large scale X-ray SASE FELs that are currently under construction [4]. However, LWFAs have not yet demonstrated sufficient quality beams to drive a viable FEL. Most notably, the measured relative energy spread is large, typically in the 2-10% range, but usually instrument resolution limited [3]. Therefore there remains a challenge to measure the energy spread with sufficient accuracy to prove the viability of the LWFA as a driver of the next generation radiation sources.

INTRODUCTION

The laser wakefield accelerator (LWFA) mechanism was first proposed thirty years ago by Tajima and Dawson [1] as an attractive alternative to RF acceleration technology. After three decades of research LWFA are now capable of producing 100s of MeV electron bunches from mm-long gas jets and, more recently, 1 GeV electron bunches have been generated from a 33 mm long discharge capillary waveguide accelerating structure [2].

The first experimental demonstration of a laser wakefield accelerator as a driver of synchrotron radiation from an undulator has recently been published [3].

EXPERIMENTAL SETUP

The experimental programme to demonstrate LWFA as drivers of compact radiation sources is currently being conducted on the Advanced Laser-Plasma High-Energy Accelerators towards X-rays (ALPHA-X) laser-wakefield accelerator beam line at the University of Strathclyde [5]. The experimental setup is shown in Fig. 1: electrons are accelerated in a relativistically self-guiding plasma channel formed in a H₂ gas jet (nozzle diameter 2 mm, plasma density $\approx 1-5 \times 10^{19} \text{ cm}^{-3}$) by Ti:sapphire laser pulses ($\lambda = 800 \text{ nm}$, energy = 900 mJ, pulse duration = 35 fs). The beam has a 40 μm $1/e^2$ spot diameter at focus and is positioned just inside the leading edge of the gas jet.

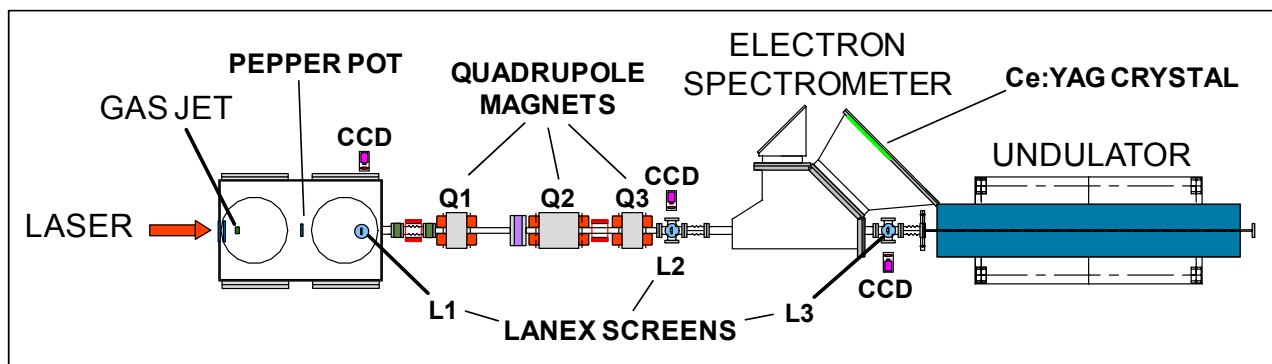


Figure 1: Setup of the ALPHA-X wakefield accelerator beam line.

Here, the peak intensity is $I = 2 \times 10^{18} \text{ W cm}^{-2}$, which gives a normalised vector potential $a_0 \approx 1$.

At these intensities electrons are self-injected from the background plasma into the plasma density wake (bubble) trailing behind the laser pulse through the combined action of the ponderomotive force of the laser and the plasma restoring force. Beams emerging from the plasma are imaged downstream using a series of pop-in Lanex scintillating screens located 0.6 m (L1), 2.2 m (L2) and 3.3 m (L3) downstream of the plasma accelerator (see Fig. 1).

A pop-in tungsten pepper-pot mask is used to measure the r.m.s. transverse emittance of the beam. This consists of a 11×11 matrix of holes with a $52 \mu\text{m}$ mean diameter. Measurements of the electron energy spectra have been carried out using a high resolution magnetic dipole spectrometer. Scintillating Ce:YAG crystals positioned at the focal plane are used to image electrons exiting the spectrometer field and the image is captured on a 12-bit CCD camera. The transportation of the beam through the spectrometer is optimised using quadrupole electromagnets (Q1, Q2 and Q3 in Fig. 1).

RESULTS

A statistical analysis of electron beam profiles recorded as CCD camera images of the L1 Lanex screen indicates that the beam is slightly elliptical in shape, with the major axis rotated 40° to the laser polarisation axis (see Fig. 2). The mean beam pointing angle is 8 mrad with respect to the laser beam axis (horizontally polarised). The angular distribution of the beam consistently consists of two superimposed approximately Gaussian distributions. A narrow diverging (~ 3 mrad) central part of the beam contains $\sim 10\%$ of the total charge while the more highly diverging (~ 30 mrad) halo comprises the remaining 90%.

Energy spectra have been measured using the spectrometer with $B = 0.59 \text{ T}$. A typical spectrum consists of a single high energy peak as shown in Fig. 3. The average central energy is $83 \pm 5 \text{ MeV}$ (that is, $\pm 6\%$ energy stability). The maximum central energy is 90 MeV. Two distinct operating modes of the spectrometer have been used to characterise the relative energy spread. Firstly, when the beam is unfocused and diverging, i.e., the quadrupole fields are turned off, [Fig. 3(a)], the average r.m.s. relative energy spread is $\sigma/\gamma = 1.7 \pm 0.3\%$ (with a minimum value of 1.2%). The high quality of the spectrum (Fig. 3) indicates that the central part of the beam (in Fig. 2) comprises a high quality electron bunch (i.e. high energy, low divergence).

With additional quadrupole focusing, beam transportation and focusing in the spectrometer is improved. In this case, $\sigma/\gamma = 1.1 \pm 0.4\%$ and the smallest value measured is 0.8% [Fig. 3(b)]. This significantly reduced energy spread demonstrates the improved beam transport using the quadrupole magnets. Since the quadrupole focusing is not quite optimal (as indicated by monitoring the beam profile), these measurements still represent an upper limit on the energy spread. Furthermore, the measured energy spread is close to the spectrometer resolution at this energy and thus the actual energy spread will need to be extracted by deconvoluting it from the instrument response profile.

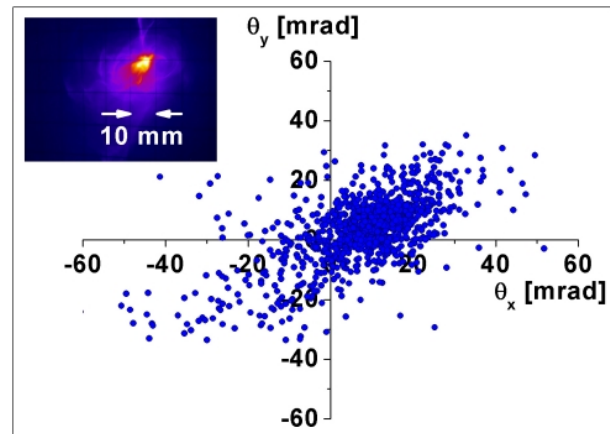


Figure 2: Angular distribution of the centroid of 1000 electron beam profiles. A typical L1 beam profile of a 3 mrad r.m.s. diverging beam is shown in the inset.

The difference in observed spectra for the different quadrupole settings is well understood because the spectrometer has been designed for a perfectly collimated beam and slight spectral broadening occurs for the divergent beam. The quadrupole magnets provide additional collimation and focusing to supplement the focusing fields of the spectrometer and obtain an optimal focus in the spectrometer focal plane.

Wakefield simulations have been carried out using a self-consistent reduced model that correctly takes into account “beam loading”, that is, local modification of the accelerating potential by the electric field of the electron bunch itself. The electron bunch length is observed to be $\sim 1 \mu\text{m}$, which is an appreciable fraction of the relativistic plasma wavelength $\lambda_p = 12 \mu\text{m}$. Without beam loading, the leading part of the electron bunch will experience a weaker acceleration field than the trailing part, which will lead to a larger energy spread (nearly 3% using

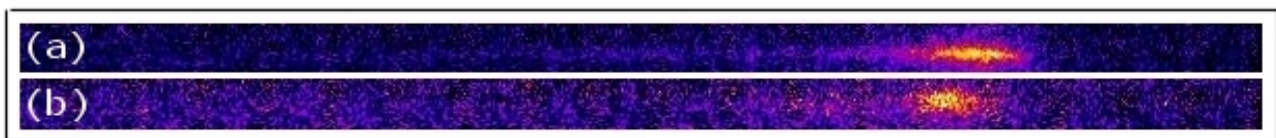


Figure 3: False colour images of representative electron spectra as captured on the YAG screen when operating (a) without and (b) with additional quadrupole fields. The energy range shown is 60 – 100 MeV (left to right).

parameters similar to those in the experiment). However, with beam loading, the electrostatic field is more uniform along the bunch length and a lower relative energy spread is obtained (close to 1%).

The normalised emittance ε_N is measured for a beam with a mean energy of 83 MeV using a pepper-pot phase space dicer. Figure 4 shows a pepper-pot image for a 4 mrad r.m.s. divergence beam and the resulting phase-space plot for the horizontal axis. This sets an upper limit for ε_N of $(5.5 \pm 1) \pi$ mm mrad, limited by the detector resolution and mask hole size. This sets a maximum source size of 18 μm , which is obviously much larger than the bubble size and therefore unrealistic. However, GPT code simulations [6] using a more appropriate source size ($\approx 3 \mu\text{m}$) indicates that a 4 mrad divergence beam would imply ε_N of the order of 0.5–1.0 π mm mrad.

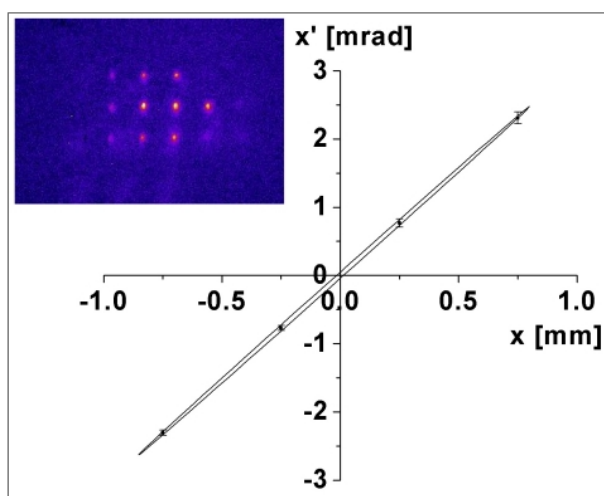


Figure 4: Phase-space diagram derived from the pepper-pot image shown in the inset.

A LWFA-DRIVEN FEL

An important application of high brightness electron beams is as a driver of a FEL. Two main criteria for obtaining FEL gain are $\sigma_{\gamma}/\gamma < \rho$ and $\varepsilon_N < \lambda\gamma/4\pi$, where ρ is the FEL gain parameter and λ is the radiation wavelength [7]. Two example scenarios are presented in Table 1 for electron beams generating spontaneous radiation in the ALPHA-X undulator [8] ($\lambda_u = 15$ mm, number of periods $N_u = 200$, $a_u = 0.38$).

Table 1: High gain FEL parameters.

Energy [MeV]	90	500
Radiation λ [nm]	260	8
ρ	0.011	0.002
σ_{γ}/γ	0.008	0.001
$\lambda\gamma/4\pi$ [mm mrad]	3.6	0.6
ε_N [mm mrad]	$\approx 1\pi$	$\approx 1\pi$

The first applies to the 90 MeV beam reported here and the second scales this to a 500 MeV electron beam from a LWFA based on a discharge capillary waveguide [2] and 10 pC of charge. It is seen that the beam quality is

close to (or may already satisfy) the requirements for net FEL gain in both cases. The peak brilliance of the radiation is $\sim 10^{30}$ photons/(s mrad² mm² 0.1% BW), estimated for a 10 fs pulse.

CONCLUSIONS

In conclusion, we have demonstrated the production of high quality electron beams from a laser wakefield accelerator. The relative energy spread of less than 1% is understood in terms of beam loading which reduces the variation of the accelerating potential over the electron bunch profile. Thus the potential is more uniform leading to a lower energy spread.

This is an important step towards the application of laser wakefield accelerators as drivers of synchrotron and FEL sources which require beams with high peak current, low emittance and low energy spread. Based on our experimental parameters, FEL gain should be observable in the deep UV wavelength range with extension into the XUV range on the horizon.

REFERENCES

- [1] T. Tajima and J. M. Dawson, Phys. Rev. Lett. 43 (1979) 267.
- [2] W. P. Leemans et al., Nature Phys. 2 (2006) 696.
- [3] H.-P. Schlenvoigt et al., Nature Phys. 4 (2008) 130.
- [4] J. Feldhaus, J. Arthur and J. B. Hastings, J. Phys. B: At. Mol. Opt. Phys. 38 (2005) S799.
- [5] D. A. Jaroszynski et al., Phil. Trans. R. Soc. A 364 (2006) 689.
- [6] S. B. van der Geer et al., 3D Space-Charge Model for GPT Simulations of High Brightness Electron Bunches, Institute of Physics Conference Series No. 175 (Institute of Physics, Bristol, UK, 2005), p. 101.
- [7] R. Bonifacio, C. Pellegrini and L. M. Narducci, Opt. Commun. 50 (1984) 373.
- [8] B. J. A. Shepherd and J. A. Clarke, Proc. EPAC'06, (2006) 3580.